https://doi.org/10.33472/AFJBS.6.11.2024.916-926

African Journal of Biological Sciences

Journal homepage: http://www.afjbs.com

Research Paper Open Access

SEED GERMINATION AND SEEDLING GROWTH RESPONSES OF PIGEON PEA (*Cajanus cajan* Linn.) OWING TO THE SUPPLEMENTATION OF A CONCOCTION OF ZnO AND α-Fe_2O_3 NANOPARTICLES

Sampa Mondal[1], Baibaswata Bhattacharjee[2*]

[1]Department of Physics, Bankura Zilla Saradamani Mahila Mahavidyapith, Bankura, WB 722101, India
[2] Department of Physics, Ramananda College, Bishnupur, Bankura, WB 722122, India

Corresponding author E-mail: [2*]baib23@gmail.com

Article Info

Volume 6, Issue 11, July 2024

Received: 23 May 2024

Accepted: 20 June 2024

Published: 09 July 2024

doi: 10.33472/AFJBS.6.11.2024.916-926

ABSTRACT:

ZnO and α-Fe_2O_3 nanoparticles are synthesized employing simple eco-friendly wet chemical methods to promote sustainable nanotechnology in agriculture. Two samples are evaluated for optical, microstructural, and compositional characteristics. These nanoparticles' impact on seed germination and plant growth promotion of Pigeon pea (*Cajanus cajan* Linn.) is assessed. With no harmful effects on seed germination, combining ZnO and α-Fe_2O_3 nanoparticles at a rate of 1:1 improves seeds' development and germination percentage. The favourable effect in seedling growth parameters (mean germination time, percentage germination, % water uptake, shoot length, and root length) and chlorophyll contents (chlorophyll a and chlorophyll b) can be associated with the increased absorption of zinc and iron in its nano form into the seed via supplements. Our findings additionally indicate that the development and germination rate of Pigeon pea become more favourable as the concentration of NPs (at a ratio of 1:1) increases up to a certain level.

Keywords: ZnO nanoparticles, α-Fe_2O_3 nanoparticles, Pigeon pea (*Cajanus cajan* Linn.), seedling growth parameters, chlorophyll contents.

1. INTRODUCTION

The current state of managing nutrition in the soil and plants is compatible with the benefits of nanotechnology. Food production and quality are significantly reduced, and human health is negatively impacted by the lack of nutrients in soils subjected to degradation and inadequate land management [1]. The nanoparticles (NPs) have a major impact on the development and promotion of seed germination [2-4]. Furthermore, because these NPs have a larger surface energy than ordinary surfaces, they may be able to aid in the delayed release of nutrients, primarily into the plant [5,6].

Numerous studies have examined the impact of zinc oxide and iron oxide NPs separately on the development, productivity, and quality of significant crops [7–10]. Plant growth metrics including plant height, branch count, and pod number are all negatively impacted by low soil zinc (Zn) availability. Zn levels in seed and tissue, as well as seed yield, are influenced by plant metabolism through decreased enzyme activity [7]. Several studies have demonstrated that treating seeds with zinc oxide causes a variety of biochemical changes in the seed that are necessary to initiate the germination process, including imbibition, enzyme activation, hydrolysis or metabolization of inhibitors, and breaking of dormancy [4]. On the other hand, several investigations have reported the impact of iron oxide NPs on the growth, production, and quality of significant crops [8]. The iron oxide NPs may induce oxidative stress in crops and change photosynthesis and mineral nutrition. Furthermore, iron oxide nanoparticles enhance agricultural growth, particularly in soils where iron is severely deficient and restricts plant physiology [8]. Enhancing food quality, decreasing negative environmental effects, and increasing nutrient efficiency are all possible by developing and applying iron oxide as nano nutrients [4]. So, individually both zinc oxide and iron oxide NPs can play a very important role in accelerating the germination process and seedling growth. In the present study, a concoction of zinc oxide and iron oxide NPs is supplemented to the seeds to acquire the combined positive impact from both the NPs in seed germination and seedling growth.

In the present research, Pigeon pea (*Cajanus cajan* Linn.) is chosen because of its nutritional significance. Furthermore, they are also the ideal source of protein supplements for diets that often consist of cereals, helping to make up for any nutritional deficiencies [11]. It is still the least utilized pulse crop in the world. In appropriate quantities, both mature and immature Pigeon pea seeds contain protein, carbs, minerals, vitamins, and vital amino acids [12]. With nutrients similar to those of corn and soybeans, Pigeon pea has the greatest potential for use as food and feed. The green leaves, roots, seeds, and pods of Pigeon pea are rich in phenolic compounds, which have the potential to treat illnesses such as measles, smallpox, chicken pox, sickle cell anemia, fever, dysentery, hepatitis, and antimalarial drugs for the body [13]. These compounds also have anti-inflammation, antibacterial, antioxidant, and antidiabetic qualities [11]. In general, Pigeon pea products like dried grain, fresh (aerial section), and green pods are utilized as an inexpensive source of high-quality and quantity of protein food and feed for the subsistence of populations living in tropical and subtropical regions. In this study, ZnO and α-Fe_2O_3 NPs (at a ratio of 1:1) are supplemented to Pigeon pea seeds at rates of zero (control), 1, 2, 3, and 4 mg/L water for 10 days. This total treatment is designed for bulk zinc oxide and iron oxide (at a ratio of 1:1) to observe the favorable effect of NPs on seedling growth parameters and chlorophyll contents. Micronutrients from ZnO NPs and α-Fe_2O_3NPs are easily absorbed by the seeds due to their nanostructure. To the best of our knowledge, this is the first report about the positive impact on the seedling growth parameters and chlorophyll contents of Pigeon pea under treatment with combined ZnO and α-Fe_2O_3NPs

(at a ratio of 1:1). In this study, the positive effects of ZnO and α-Fe_2O_3NPs on seedling growth parameters (mean germination time, percentage germination, % water uptake, shoot length, and root length) and chlorophyll contents (chlorophyll a and chlorophyll b) has been studied systematically. Under the same conditions, seedling growth parameters and chlorophyll contents of Pigeon pea seed differ significantly with varying concentrations of NPs. Our results also show that, up to a certain point, seedling growth parameters and chlorophyll contents of Pigeon pea get more favorable when the concentration of NPs rises because of nano-supplementation.

2. EXPERIMENTAL DETAILS

2.1. Synthesis of ZnO NPs

At first, under continual stirring at room temperature, 12.5 gm of Zinc nitrate hexahydrate ($Zn(NO_3)_2 \cdot 6H_2O$) (Sigma-Aldrich, purity 99%) and 4.50 gm of potassium hydroxide (KOH) (Sigma-Aldrich, purity 99.99%) are dissolved in 250 mL and 200 mL of distilled deionized (DI) water. KOH solution is then dropped into the Zn $(NO_3)_2 \cdot 6H_2O$ solution, and the resulting milky white solution with no precipitation is stirred for 4 hours at room temperature. The solution is filtered with Whatman No. 1 filter paper and dried at 90°C in the open air after being washed five times with DI water. Finally, the dried sample is annealed at 350°C in an air atmosphere for 3 hours to get ZnO NPs in powder form.

2.2. Synthesis of α-Fe_2O_3 NPs

Firstly, 3.5 gm of ferric chloride hexahydrate ($FeCl_3 \cdot 6H_2O$) (Merck, purity 99.99%) is dissolved in 250 ml of DI water under continual stirring at room temperature. Separately, 2.2 gm of sodium hydroxide (NaOH) (Sigma-Aldrich, purity 99.99%) is dissolved in 250 mL of DI water under vigorous stirring at room temperature. After that, the NaOH solution is mixed dropwise into the $FeCl_3 \cdot 6H_2O$ solution. The resulting reddish-black solution is stirred for an additional 5 hours at 90 °C. This solution is then filtered to obtain the precipitates, which are washed four times with DI water. The precipitates are then heated at 100 °C until they become completely dry. After that, the dried samples are annealed in a muffle furnace for 3 hours at 250 °C. Finally, the samples are grounded to obtain the samples in the form of fine powder.

2.3. Characterizations and Instrumentations

Using a Bruker D8 Advance diffractometer, the crystallinity of the ZnO and α-Fe_2O_3 NPs is assessed throughout an angular range (2θ) of 20-80°. A Zeiss Sigma field-enhanced secondary electron microscope (FESEM) is used to examine the morphology of the produced NPs. A Jasco V-770 spectrophotometer is used to record UV-VIS absorption spectra spanning the wavelength range of 300-1000 nm.

2.4. Experimental exposure of seed germination

In this research, a combination of ZnO NPs and α-Fe_2O_3 NPs are added to the Pigeon pea seeds at different ratios (at 1:3, 1:2, 1:1, 2:1, and 3:1 ratio) for different concentrations (1, 2, 3, and 4 mg/L water) to optimize the favorable effect for the combination of NPs. It has been observed that the most positive impact has been seen in seeds for a 1:1 nanoparticle ratio. So, in this report, the positive effects in Pigeon pea seed germination for the combination of ZnO NPs and α-Fe_2O_3 NPs (at a 1:1 ratio) are discussed in detail. The study examines the changes in seed for 4 distinct concentrations of NPs compared to the control group. The ZnO NPs and α-Fe_2O_3 NPs (at a 1:1 ratio) are given to the seeds at rates of zero (control), 1, 2, 3, and 4 mg/L water for 10 days (Table 1). This full treatment is also designed for bulk zinc oxide and iron oxide (at a 1:1 ratio) to compare the effects of NPs. 10 seeds of the same size are put into each of the 100 ×15 mm Petri dishes that have two layers of sterilized filter paper lining them. 5 ml of sterile distilled water is used to wet the filter paper for the control

group. At a time, 2.5 ml of ZnO NPs and α-Fe_2O_3 NPs are given to the Petri dishes by the experimental design (Table 1). The treatment with bulk zinc oxide and iron oxide also maintains this process. They are then incubated for ten days at 30 ± 1° C. The same volume of treatment solution was added each day to prevent drying, and each treatment was run through three replicates. Four days after the incubation process the percentage of germination is measured. The Petri dishes are taken out after 10 days, and the fresh weight, dry weight, % water uptake, shoot length, root length, chlorophyll a, and chlorophyll b measurements are made.

Table 1. Included ZnO and α-Fe_2O_3 NPs samples supplement for different experimental groups.

Experimental groups	Included nanoparticles supplement according to concentration (mg/ L water)
Control group	0
Treatment 1	1
Treatment 2	2
Treatment 3	3
Treatment 4	4

2.5. Determination of Chlorophyll contents in the plant leaves

The technique of [14] is used to determine total chlorophyll. Using a spectrophotometer, 50 mg of fresh leaf material is manually homogenized in 10 ml of 80% acetone, and the absorbance is measured at 645 and 663 nm.

3. RESULTS AND DISCUSSION

3.1. X-ray diffraction (XRD)

The XRD spectra of ZnO NPs and α-Fe_2O_3 NPs are shown in Figure 1. The nature of the peaks is found to be broad depicting the nanoparticle nature of the samples. However, the ZnO sample exhibits common peaks located at 2θ positions of 31.84°, 34.45°, 36.28°, 47.55°, 56.64°, 62.84°, 66.47°, 67.96°, 69.20°, 72.64°, 76.94° which are attributed to the crystal planes 100, 002, 101, 012, 110, 013, 200, 112, 201, 004, and 011, respectively, where ZnO NPs has a hexagonal crystal structure (Figure 1a) [15]. On the other hand, the presented picks for the α-Fe_2O_3 sample match the (012), (104), (110), (113), (024), (116), (214), and (300) of a hexagonal structure of α- Fe_2O_3 NPs, identified using standard data (JCPDS 33-0664) (Figure 1b) [16].

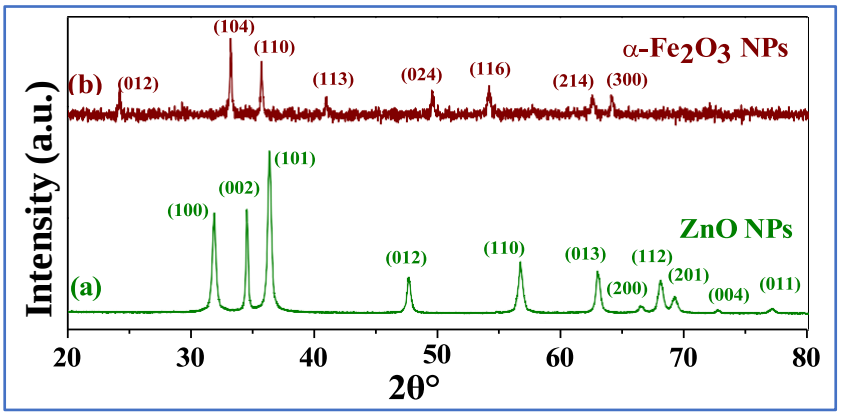

Figure 1. XRD patterns of NPs: (a) ZnO NPs, (b) α-Fe_2O_3 NPs.

The mean sizes of the NPs are determined using the Debye-Sherrer formula and the following equation [17–20]:

$$D = \frac{0.89\,\lambda}{\beta\,cos\theta} \quad (1)$$

Where λ is the wavelength of the X-ray used (here λ=1.54 Aº for Cu K_α radiation), θ is the Bragg angle, the full width at half maximum (FWHM) of the X-ray diffraction peak is β and the shape factor is 0.89. The mean particle sizes of ZnO and α- Fe_2O_3 samples are given in Table 2.

3.2. Morphological Investigation

The particle size and particle size distribution of ZnO and α- Fe_2O_3 NPs are investigated using the FESEM micrographs. The FESEM images of ZnO and α- Fe_2O_3 NPs are displayed in Figure 2. The shape of the majority of ZnO NPs is found to be spherical or spheroidal (Figure 2a). The shapes of the majority of α-Fe_2O_3 NPs are found to be spherical or oval (Figure 2b). Figure 2a (inset) and Figure 2b (inset) show the particle size distribution histogram that is obtained from the corresponding FESEM images along with the theoretical curves fitted with the particle size distribution data. The particle sizes are found to follow the log-normal distribution pattern, which is common for samples containing very small particles. The average particle sizes estimated through morphological investigation are displayed in Table 2.

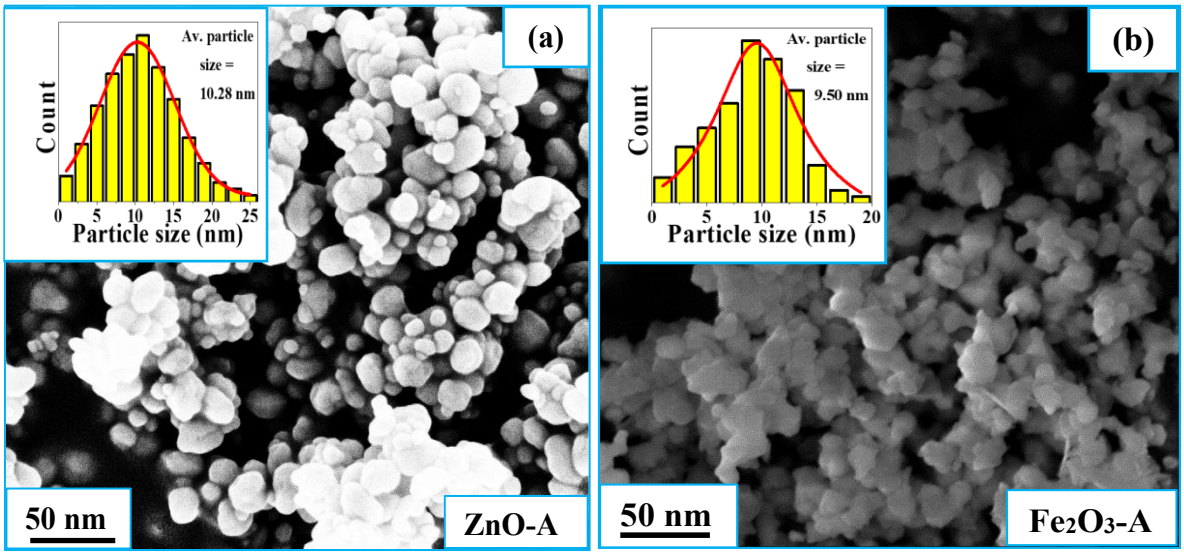

Figure 2. FESEM images with corresponding particle size distribution histograms of NPs: (a) ZnO NPs, (b) α-Fe_2O_3 NPs.

3.3. UV-VIS spectroscopy

The absorption spectra of the produced ZnO and α-Fe_2O_3 NPs are shown in Figure 3. The optical bandgaps of the as-prepared NPs are estimated using the Tauc plot by plotting $(\alpha h\nu)^2$ against hν and extrapolating the band edge slope against zero [21–23]. The estimated optical bandgaps of NPs are given in Table 2. However, the lower band gap value of ZnO NPs compared to bulk materials (3.3 eV) can be attributed to planar defect (Table 2) [19].

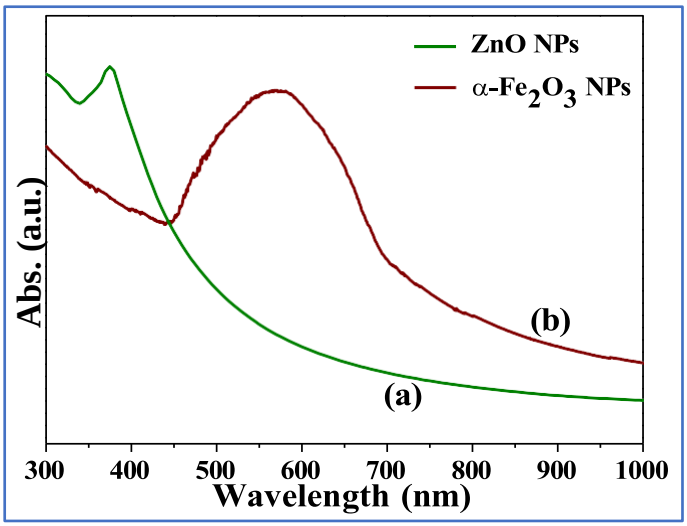

Figure 3. UV-VIS absorption spectrum of NPs: (a) ZnO NPs, (b) α-Fe_2O_3 NPs.

Table 2. Estimated particle size from XRD and SEM, and energy band gap of ZnO NPs and α-Fe_2O_3 NPs.

Sample Name	Average Particle size (nm) from XRD	Average Particle size (nm) from SEM	Band gap energy (eV)
ZnO NPs	10.42	10.28	3.27
α-Fe_2O_3 NPs	8	8.02	2.90

3.4. Seed germination studies

Several studies have demonstrated that treating seeds with zinc (Zn) causes a variety of biochemical changes in the seed that are necessary to initiate the germination process, including imbibition, enzyme activation, hydrolysis or metabolization of inhibitors, and breaking of dormancy [4]. On the other hand, several investigations have reported the impact of iron oxide NPs on the growth, production, and quality of significant crops [8]. So, the values of seedling growth parameters (mean germination time, percentage germination, % water uptake, shoot length, and root length) of Pigeon pea seeds are changed by adding a mixture of ZnO NPs and α-Fe_2O_3 NPs supplements at a 1:1 ratio.

Further, mean germination time (MGT) and % water uptake (WUT) are calculated using standard formulations [24,25].

$$MGT = \frac{\sum N \times t}{\sum N} \quad (2)$$

$$WUT\ (\%) = \frac{(Freash\ weight\ of\ seed - dry\ weight\ of\ seed) \times 100}{dry\ weight\ of\ seed} \quad (3)$$

Where N is the number of germinated seeds and t is hours from the beginning of the germination test.

Figures 4a, 4b, 4c, 4d, and 4e show the changes in mean germination time, percentage germination, % water uptake, shoot length, and root length respectively with concentration for different experimental groups.

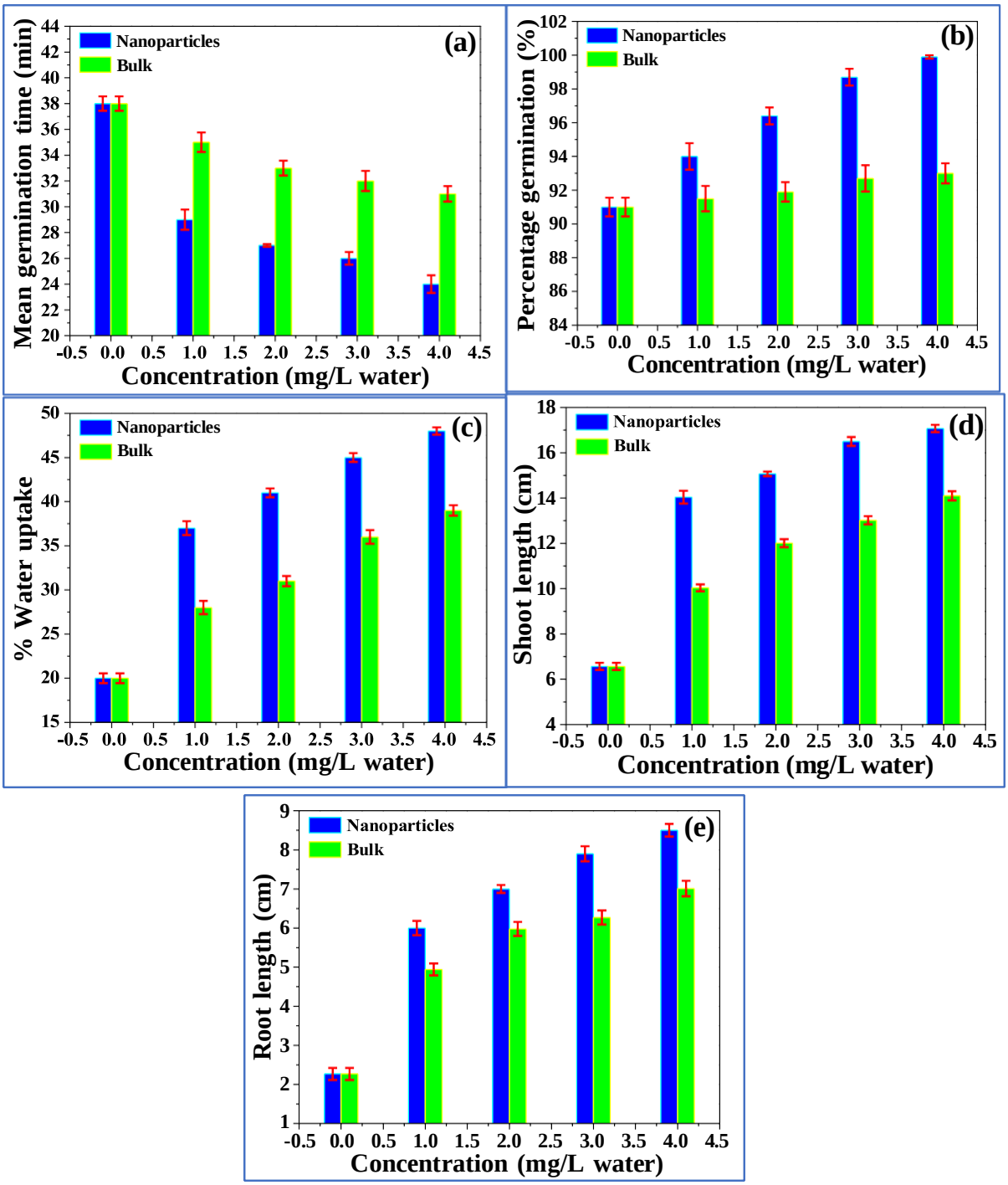

Figure 4. Variation of seedling growth parameters of Pigeon pea under different experimental designs with increasing concentration of zinc oxide and iron oxide (at 1:1 ratio) along with control group: (a) mean germination time, (b) percentage germination, (c) % water uptake, (d) shoot length, (e) root length.

Figure 4a shows that MGT decreases with rising concentrations of zinc oxide and iron oxide. The control group has a maximum MGT (38 min). The treatment with NPS at 4 mg/L water has the lowest MGT (24 min) (Figure 4a). The germination percentage, % water uptake, shoot length, and root length increase with increasing concentrations of zinc oxide and iron oxide (at a 1:1 ratio). The control group has the lowest value for these parameters (Figure 4b-4e). The treatments show that maximum value of germination percentage, % water uptake, shoot length, and root length at about 99.9 % (Figure 4b), 48 % (Figure 4c), 17.07 cm (Figure 4d) 8.5 cm (Figure 4e) respectively are observed for NPs (ZnO:α-Fe_2O_3= 1:1) at 4 mg/L water concentration. Additionally, it is observed that these positive impacts to promote seed germination become less effective

under treatment groups with bulk zinc oxide and iron oxide (at a 1:1 ratio).

3.5. Measurement of chlorophyll contents

The chlorophyll contents of Pigeon pea under different experimental conditions are investigated using UV-Vis spectra of chlorophyll of Pigeon pea leaves. Here, the absorption spectra of chlorophyll of Pigeon pea leaves under treatment 4 is shown in Figure 5a as a representative. The absorption spectra and their corresponding deconvoluted Gaussian fitted peaks of chlorophyll of Pigeon pea leaves under treatment 4 for the blue and red regions are displayed in Figures 5b and 5c respectively. In this study, chlorophyll contents of Pigeon pea leaves are measured using absorption spectra for the red region (absorbance at 645 and 663 nm) (Fig 5c) because this is a standard method used by other researchers [26].

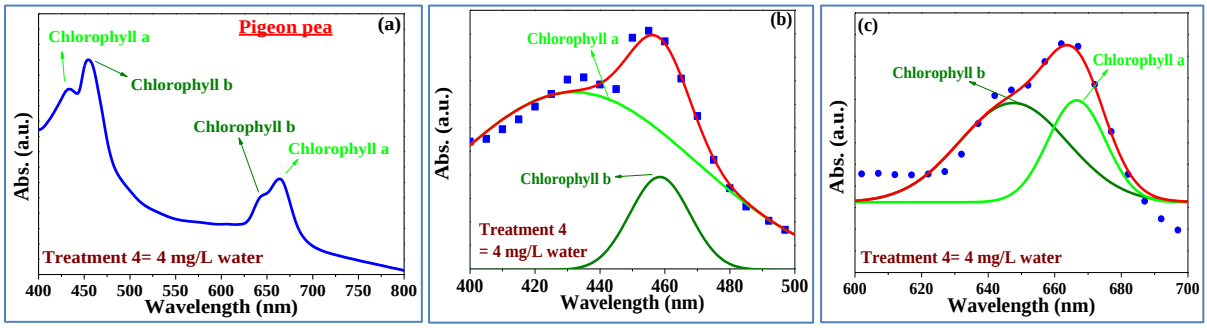

Figure 5. (a) UV-Vis spectra of chlorophyll contents of Pigeon pea leaves under treatment 4 (zinc oxide and iron oxide NPs at 1:1 ratio), (a) UV-Vis spectra and their corresponding deconvoluted Gaussian fitted peaks of chlorophyll contents of Pigeon pea leaves under treatment 4 for the blue region, (b) UV-Vis spectra and, their corresponding deconvoluted Gaussian fitted peaks of chlorophyll contents of Pigeon pea leaves under treatment 4 for red region.

The chlorophyll contents of Pigeon pea leaves are estimated using the following formulas [26]:

$$Chlorophyll\ a\ (mg/g) = 12.7\ (A_{663}) - 2.69\ (A_{645}) \times \frac{V}{1000 \times W} \quad (3)$$

$$Chlorophyll\ b\ (mg/g) = 22.9\ (A_{645}) - 4.68\ (A_{663}) \times \frac{V}{1000 \times W} \quad (4)$$

Where A is the absorbance at a particular wavelength as mentioned in the equation, V is the final volume of the sample made, and W is the fresh weight of the sample taken.

Figures 6a and 6b show that chlorophyll a and chlorophyll b of Pigeon pea leaves increase as the concentration of NPs increases for different experimental groups.

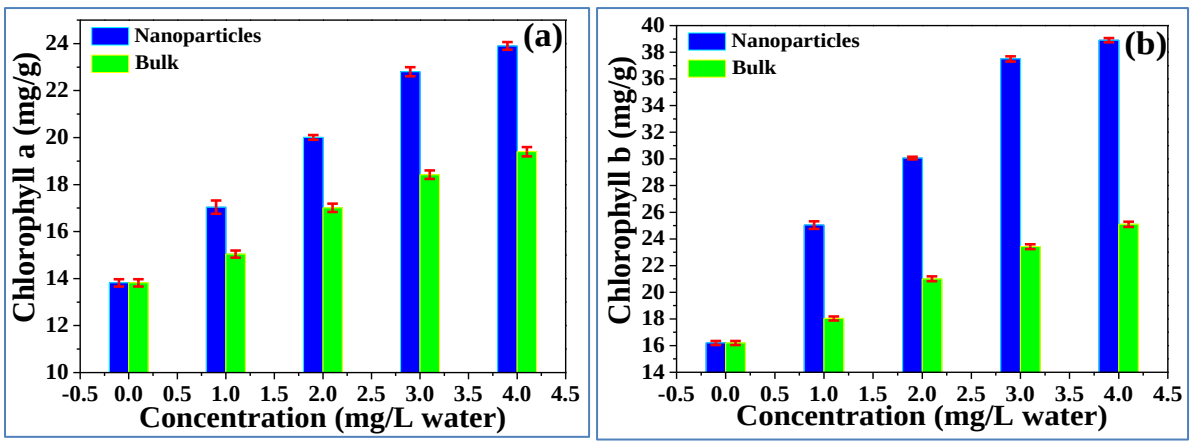

Figure 6. Variation of chlorophyll contents of Pigeon pea leaves under different experimental designs with increasing concentrations of zinc oxide and iron oxide (at 1:1 ratio) along with the control group: (a) chlorophyll a, (b) chlorophyll b.

The control group has the minimum chlorophyll contents. The treatments show that maximum chlorophyll a and chlorophyll b at about 23.88 mg/g (Figure 6a), and 38.9 mg/g (Figure 6b) respectively are seen for NPs (ZnO:α-Fe_2O_3= 1:1) at 4 mg/L water concentration. Furthermore, the amount of chlorophyll contents in Pigeon pea leaves is seen to decrease in treatment groups treated with bulk zinc oxide and iron oxide (at a 1:1 ratio).

4. CONCLUSION

Simple and low-cost wet chemical methods have been used to produce high-grade, pure, highly crystalline wurtzite-structured ZnO NPs and α-Fe_2O_3 NPs. SEM and XRD investigations confirm that excellent ZnO NPs and α-Fe_2O_3 NPs are produced. The mixture of ZnO NPs and α-Fe_2O_3 NPs at a ratio of 1:1 is employed as a supplement at rates of zero (control), 1, 2, 3, and 4 mg/L water for 10 days for enhancing germination parameters and chlorophyll contents of nutritionally significant Pigeon pea (*Cajanus cajan* Linn.). To examine the beneficial effects of NPs on seedling growth parameters (mean germination time, percentage germination, % water uptake, shoot length, and root length) and chlorophyll contents (chlorophyll a and chlorophyll b) of Pigeon pea, this entire treatment is designed for bulk and NPs at a ratio of 1:1 for different concentrations. The study shows that the mean germination time of Pigeon pea seeds is the lowest (24 min) for treatment with NPs (ZnO:α-Fe_2O_3= 1:1) at 4 mg/L water concentration. The treatment has resulted in a notable enhancement of the percentage germination, % water uptake, shoot length, root length, chlorophyll a, and chlorophyll b. When the concentration of NPs rises to 4 mg/L water, the value of percentage germination, % water uptake, shoot length, root length, chlorophyll a, and chlorophyll b increase. When comparing the positive impact of NPs (ZnO:α-Fe_2O_3= 1:1) to the control group, the treatments indicate that at 4 mg/L water, percentage germination, % water uptake, shoot length, root length, chlorophyll a and chlorophyll b of Pigeon pea pointedly increase from 91% to 99.9%, from 20 % to 48%, from 6.57 cm to 17.07 cm, from 2.27 cm to 8.5 cm, from 13.82 mg/g to 23.88 mg/g, and from 16.2 mg/g to 38.9 mg/g, respectively. Thus, our study also offers a simple and easy way to enhance the germination process of Pigeon pea seeds.

ACKNOWLEDGEMENTS

The authors would like to acknowledge the Co-Ordinator, Centre of Excellence in Advanced Materials, National Institute of Technology Durgapur, for microstructural characterization.

FUNDING

This research did not receive any specific grant from funding agencies in public, commercial, or not-for-profit sectors.

DECLARATIONS

Conflict of Interest The authors declare no competing interests.

REFERENCES

[1] Tovar GI, Briceño S, Suarez J, Flores S, González G. Biogenic synthesis of iron oxide nanoparticles using Moringa oleifera and chitosan and its evaluation on corn germination. Environ Nanotechnol Monit Manag 2020;14:100350. https://doi.org/10.1016/j.enmm.2020.100350.

[2] E. U. E, P. C. Assessment of phytoremediation potential of cowpea (Vigna unguiculata L Walp) on used motor oil contaminated soil. Afr J Biol Sci 2021;3:29. https://doi.org/10.33472/AFJBS.3.3.2021.29-36.

[3] Epee Misse PT. Dormancy and germination in two Australian native species (Acacia aneura and Rhodanthe floribunda). Afr J Biol Sci 2019;01:55. https://doi.org/10.33472/AFJBS.1.2.2019.55-59.

[4] Awan S, Shahzadi K, Javad S, Tariq A, Ahmad A, Ilyas S. A preliminary study of influence of zinc oxide nanoparticles on growth parameters of Brassica oleracea var italic. J Saudi Soc Agric Sci 2021;20:18–24. https://doi.org/10.1016/j.jssas.2020.10.003.

[5] Itroutwar PD, Kasivelu G, Raguraman V, Malaichamy K, Sevathapandian SK. Effects of biogenic zinc oxide nanoparticles on seed germination and seedling vigor of maize (Zea mays). Biocatal Agric Biotechnol 2020;29:101778. https://doi.org/10.1016/j.bcab.2020.101778.

[6] Tombuloglu G, Aldahnem A, Tombuloglu H, Slimani Y, Akhtar S, Hakeem KR, et al. Uptake and bioaccumulation of iron oxide nanoparticles (Fe3O4) in barley (Hordeum vulgare L.): effect of particle-size. Environ Sci Pollut Res 2024;31:22171–86. https://doi.org/10.1007/s11356-024-32378-y.

[7] Yadav A, Babu S, Krishnan P, Kaur B, Bana RS, Chakraborty D, et al. Zinc oxide and ferric oxide nanoparticles combination increase plant growth, yield, and quality of soybean under semiarid region. Chemosphere 2024;352:141432. https://doi.org/10.1016/j.chemosphere.2024.141432.

[8] Lin T, Chen X, Ren Y, Qing B, Zhang M, Mo Z, et al. Effects of iron oxide nanocoatings on the seed germination, seedling growth, and antioxidant response of aromatic rice grown in the presence of different concentrations of rice straw extracts. J Nanoparticle Res 2024;26:78. https://doi.org/10.1007/s11051-024-05986-5.

[9] Dahiru MB, Yarima A, Abubakar AI, Abubakar ZA. Mutagenic effects of sodium azide on some qualitative traits of maize (Zea mays). Afr J Biol Sci 2021;3:34–51. https://doi.org/10.33472/AFJBS.3.1.2021.52-57.

[10] Al-huraby AI, Bafeel SO. The effect of salinity stress on the Phaseolus vulgaris L. plant. Afr J Biol Sci 2022;4:94. https://doi.org/10.33472/AFJBS.4.1.2022.94-107.

[11] Fatokimi EO, Tanimonure VA. Analysis of the current situation and future outlooks for pigeon pea (Cajanus Cajan) production in Oyo State, Nigeria: A Markov Chain model approach. J Agric Food Res 2021;6:100218. https://doi.org/10.1016/j.jafr.2021.100218.

[12] Haji A, Teka TA, Yirga Bereka T, Negasa Andersa K, Desalegn Nekera K, Geleta Abdi G, et al. Nutritional Composition, Bioactive Compounds, Food Applications, and Health Benefits of Pigeon Pea (*CAJANUS CAJAN* L. Millsp.): A Review. Legume Sci 2024;6:e233. https://doi.org/10.1002/leg3.233.

[13] Wu J, Zhou Q, Zhou C, Cheng K, Wang M. Strategies to promote the dietary use of pigeon pea (*Cajanus cajan* L.) for human nutrition and health. Food Front 2024;5:1014–30. https://doi.org/10.1002/fft2.381.

[14] Marcu D, Damian G, Cosma C, Cristea V. Gamma radiation effects on seed germination, growth and pigment content, and ESR study of induced free radicals in maize (Zea mays). J Biol Phys 2013;39:625–34. https://doi.org/10.1007/s10867-013-9322-z.

[15] Gherbi B, Laouini SE, Meneceur S, Bouafia A, Hemmami H, Tedjani ML, et al. Effect of pH Value on the Bandgap Energy and Particles Size for Biosynthesis of ZnO Nanoparticles: Efficiency for Photocatalytic Adsorption of Methyl Orange. Sustainability 2022;14:11300. https://doi.org/10.3390/su141811300.

[16] Rao X, Su X, Yang C, Wang J, Zhen X, Ling D. From spindle-like β-FeOOH nanoparticles to α-Fe2O3 polyhedral crystals: shape evolution, growth mechanism and gas sensing property. CrystEngComm 2013;15:7250. https://doi.org/10.1039/c3ce40430g.

[17] Masoumi M, Rahmati S, Saraiva BRc, Marçal LAb, Béreš M, De Abreu HFg. High-pressure phase transformations and lattice distortions in industrial AISI 1070 steel: Insights from Debye-Scherrer ring integration. Mater Sci Eng A 2024;897:146363. https://doi.org/10.1016/j.msea.2024.146363.

[18] Aydin Yuksel S, Gul EM, Senberber Dumanli FT, Derun EM. Ultrasonic-assisted Co-precipitation synthesis of CoAl2O4 with different capping agents: Determination of electrical and optical features. Mater Chem Phys 2024;313:128706. https://doi.org/10.1016/j.matchemphys.2023.128706.

[19] Jalali T, Ghanavati F, Osfouri S. Green synthesis of ZnO nanoparticles using marine brown algae (*Cystoseira*) extract comprising sol–gel, and combustion techniques based on dye-sensitized solar cells application. Int J Mod Phys B 2024;38:2450178. https://doi.org/10.1142/S0217979224501789.

[20] Eslami A, Lachini SA, Shaterian M, Karami M, Enhessari M. Sol-gel synthesis, characterization, and electrochemical evaluation of magnesium aluminate spinel nanoparticles for high-capacity hydrogen storage. J Sol-Gel Sci Technol 2024;109:215–25. https://doi.org/10.1007/s10971-023-06260-1.

[21] Ghazy AR, Shalaby MG, Ibrahim A, ElShaer A, Mahmoud YA-G, Al-Hossainy AF. Synthesis, structural and optical properties of Fungal biosynthesized Cu2O nanoparticles doped Poly methyl methacrylate -co-Acrylonitrile copolymer nanocomposite films using experimental data and TD-DFT/DMOl3 computations. J Mol Struct 2022;1269:133776. https://doi.org/10.1016/j.molstruc.2022.133776.

[22] Ibrahim M, Saron KMA, Ghalab S, Asnag GM, Morsi MA, Tarabiah AE. Study of the structural, optical and electrical properties of PVA/SA performance by incorporating Al2O3 nanoparticles. Opt Quantum Electron 2024;56:979. https://doi.org/10.1007/s11082-024-06916-4.

[23] Gholizadeh Z, Aliannezhadi M, Ghominejad M, Shariatmadar Tehrani F. Optical and structural properties of spherical-shaped boehmite and γ-alumina nanoparticles by ultrasonic-assisted hydrothermal method: the effects of synthesis route, calcination, and precursor concentration. Opt Quantum Electron 2023;55:880. https://doi.org/10.1007/s11082-023-05157-1.

[24] Sharma N, Sinha VB, Gupta N, Rajpal S, Kuchi S, Sitaramam V, et al. Phenotyping for Nitrogen Use Efficiency: Rice Genotypes Differ in N-Responsive Germination, Oxygen Consumption, Seed Urease Activities, Root Growth, Crop Duration, and Yield at Low N. Front Plant Sci 2018;9:1452. https://doi.org/10.3389/fpls.2018.01452.

[25] Afsheen S, Naseer H, Iqbal T, Abrar M, Bashir A, Ijaz M. Synthesis and characterization of metal sulphide nanoparticles to investigate the effect of nanoparticles on germination of soybean and wheat seeds. Mater Chem Phys 2020;252:123216. https://doi.org/10.1016/j.matchemphys.2020.123216.

[26] Wadas W, Dziugieł T. Changes in Assimilation Area and Chlorophyll Content of Very Early Potato (Solanum tuberosum L.) Cultivars as Influenced by Biostimulants. Agronomy 2020;10:387. https://doi.org/10.3390/agronomy1003038.